Acc. Chem. Res. **1998,** *31,* 289−296

Surface Acoustic Wave Chemical Sensor Arrays: New Chemically Sensitive Interfaces Combined with Novel Cluster Analysis To Detect Volatile Organic Compounds and Mixtures

ANTONIO J. RICCO,*,† RICHARD M. CROOKS,*,‡ AND GORDON C. OSBOURN*,§

Microsensor R&D and Vision Science Departments, Sandia National Laboratories, Albuquerque, New Mexico 87185-1425, and Department of Chemistry, Texas A&M University, College Station, Texas 77843-3255

Received June 24, 1997

Three approaches confer chemical selectivity upon a sensor-based system.[1] The "traditional" approach uses a single sensor functionalized with a chemically sensitive material selective for the analyte. This works well when interferences are few, or chemically unlike the analyte, or when highly specific materials—e.g., suitable biological or molecular-recognition complexes—are available. Even with exquisite selectivity, the transducer platform often must include a physical selectivity mechanism as well, so that nonspecific adsorption does not defeat a carefully crafted interface. An example is wavelength-specific optical detection that can differentiate between analytes physisorbed on the surfaces of a molecular cage and those residing inside. In contrast, a "nonspecific" transducer such as the mass-sensitive surface acoustic wave (SAW) device cannot differentiate between physisorbed and molecularly complexed mass on the surface of a device, unless a secondary perturbation such as a change in mechanical or electrical properties accompanies the mass change.[2]

Recent advances in both miniaturized and "micro" versions of traditional analytical techniques drive a second approach to chemical selectivity, that of separating analytes in time, space, or the spectral domain.[3−5] Typified by electrophoretic separations in microfabricated channels on glass chips, the micro-total-analytical system (μ-TAS) approach can diminish the role of the sensor to that of a nonspecific detector that responds to any impinging compound. The elapsed time from sample introduction to detection, rather than detector selectivity, identifies the analyte.

We focus in this Account on chemical sensor arrays as a means to obviate the difficult, costly process of developing a new material with high chemical specificity for each analyte: one array can provide distinct responses for tens of chemicals and mixtures. We emphasize that many of the subsections of this Account are, to varying degree, "platform independent", so that arrays of optical fibers, electrochemical sensors, chemiresistors, metal oxides, or thermal devices can be conceptually substituted for the SAW platforms that we discuss in detail. The moderate selectivity requirements for arrays allow consideration of a much wider range of materials—everything from common organic polymers to porous ceramics—than for molecularly specific sensors. Furthermore, arrays retain some of the "passive sampling" features of discrete sensors that μ-TAS must relinquish due to its reliance upon addition of reagents, pumping, mixing, and the like.

Selecting Interface Materials: Chemical Independence

When the goal is to produce a chemical sensor array that responds uniquely to each of many analytes, chemical diversity is key to the selection of interfacial materials. The fundamental research and preliminary development of acoustic wave chemical sensors has included an encouragingly diverse collection of chemically sensitive interface materials (see ref 2, Chapter 5, and references therein): metal films; ceramics; organic, organometallic, and inor-

Antonio J. Ricco was born in Oakland, CA, in 1958. He received a B.S. in chemistry (magna cum laude) from the University of California, Berkeley, in 1980 and a Ph.D. in inorganic chemistry from the Massachusetts Institute of Technology in 1984. He joined Sandia National Laboratories' Microsensor Research Division in 1984, where his research currently involves chemical sensor arrays based on acoustic wave, optical, electrochemical, chemiresistor, and microelectronic platforms. His research focuses on new ways to utilize chemical and physical effects together with new materials in combination with microelectronic technology and pattern recognition to develop novel chemical sensors with enhanced capabilities.

Richard M. Crooks received his Bachelor of Science degree in chemistry from the University of Illinois (Urbana, IL) and his doctoral degree in electrochemistry from the University of Texas (Austin, TX) in 1987. He is currently Professor of Chemistry at Texas A&M University (College Station, TX). His research interests include chemical sensors and interfacial design, electrocatalysis, corrosion and corrosion inhibition, physical electrochemistry, and the molecular basis of adhesion and adhesive interactions.

Gordon C. Osbourn received the B.S. degree in physics and mathematics in 1974 and the M.S. degree in physics in 1975 from the University of Missouri at Kansas City and the Ph.D. degree in physics in 1979 from the California Institute of Technology. He joined the technical staff of Sandia National Laboratories in 1979 and is currently Manager of the Vision Science, Pattern Recognition and Multisensor Algorithm Department. Osbourn was selected as 1 of 100 outstanding young U.S. scientists by *Science Digest* in 1984. He received the 1985 Department of Energy E. O. Lawrence award and the 1993 American Physical Society International Prize for New Materials for initiating the study of a new class of semiconductor quantum wells and superlattices. He has coauthored 75 publications and has been awarded 6 patents on semiconductor devices and 1 patent on image processing. He is a fellow of the American Physical Society and a member of the Optical Society of America. His current research interests include the study of human vision, the development of robust pattern recognition and clustering algorithms, and multivariate image classification applications and the application of those techniques to chemical sensing problems.

* Address correspondence to any author.
† Microsensor R&D Department, Sandia National Laboratories.
‡ Texas A&M University.
§ Vision Science Department, Sandia National Laboratories.

S0001-4842(96)00074-X CCC: $15.00
Published on Web 05/02/1998

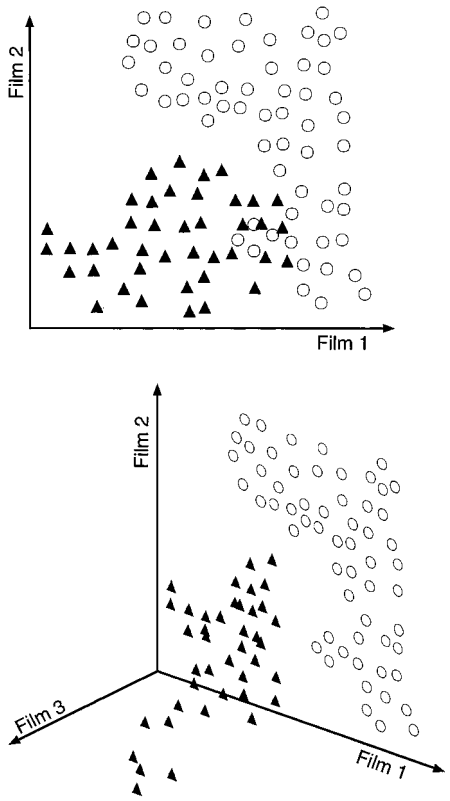

FIGURE 1. Hypothetical response of a sensor array to two analytes, represented by open circles and filled triangles. At the top, the responses of films 1 and 2 clearly show a number of concentrations where responses to the two analytes overlap and errors in identification are inevitable. At the bottom, the response of film 3 separates the two sets of responses in the overlap region. Film 3 is chemically independent of films 1 and 2.

ganic semiconductors; organometallic compounds and coordination complexes; organic oils and waxes; and a vast collection of organic polymers. Pioneering work on the effective combination of SAW arrays with organic polymer films began in the mid-1980s at the Naval Research Laboratory.[6,7] Designing a sensor array for a particular application should include the evaluation of coatings from many categories, rather than being restricted to a single class of material. We present results below to support the claim that materials diversity leads to more effective arrays. Assuming a range of thin films is available, two difficult questions remain: How many sensors should comprise the array, and which films should be selected? The answers depend critically upon the application, but there are important general considerations.

For any sensor array, *chemical independence* of interface materials is critical: no film's response should be predictable from those of the other films in the array. For example, consider an array composed of two thin-film-coated sensors (films 1 and 2) for the detection of analytes A and B (discrete compounds or chemical mixtures). If some concentrations of A and B elicit a very similar response from both films, mistakes are bound to be made in identifying the analytes.[8] This situation, represented graphically in the top panel of Figure 1, motivates a search

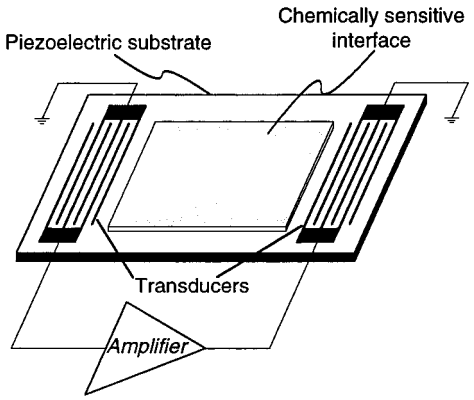

FIGURE 2. Surface acoustic wave (SAW) delay line with a chemically sensitive interface layer and basic oscillator circuit.

for some film 3, whose response is chemically independent of films 1 and 2, and which eliminates response overlap.

The bottom panel of Figure 2 shows the results of choosing an appropriate film 3. In the critical region where analytes A and B's responses overlap in the top panel, the new film has added an axis which effectively separates analytes A and B; film 3 is chemically independent of films 1 and 2.

The concepts of chemical and linear independence should not be confused. To illustrate, we postulate the physical mixture of two sensor materials (films 1 and 2) to create a new material (film 4) whose response is found *not* to be a linear combination of the two components, due to a cross-term:

$$R_{4,A} = a_1R_{1,A} + a_2R_{2,A} + a_3R_{1,A}R_{2,A} \quad (1)$$

$$R_{4,B} = b_1R_{1,B} + b_2R_{2,B} + b_3R_{1,B}R_{2,B} \quad (2)$$

Here $R_{i,A}$ and $R_{i,B}$ are functions that designate the respective concentration-dependent responses of film i to analytes A and B; a_i and b_i are scalar coefficients. Clearly, the response of film 4 is *linearly* independent of films 1 and 2. However, in the event that $a_i = b_i$ for all i, film 4 is *not chemically* independent of films 1 and 2, and film 4 will give equal responses to analytes A and B whenever films 1 and 2 do, e.g., in an overlap region like that in the top panel of Figure 1. Therefore, film 4 provides no additional chemical information. The need for inequality of the a_i and b_i should be considered qualitatively: the more disparate the response of film 4 to analytes A and B, in light of the known responses of films 1 and 2, the more new information is provided by film 4.

Case Study: Self-Assembled Monolayers and Plasma-Processed Films

Consistent with the goal of chemical diversity, we have examined a range of materials from which sensor coatings might be formed, including alkanethiol-based self-assembled monolayers (SAMs),[9,10] plasma-polymerized films (PPFs) and plasma-grafted films (PGFs),[1,11] custom-synthesized conventional polymers,[12] thin films based on dendrimeric polymers,[13] metal thin films,[14] organometallic

Table 1. Analytes Arranged by Chemical Class

chemical class	compounds studied		
aliphatic hydrocarbon	cyclohexane	isooctane[b]	kerosene[a]
aromatic hydrocarbon	benzene	toluene[b]	
chlorinated hydrocarbon	carbon tetrachloride	trichloroethylene[b] (TCE)	
alcohol	methanol	1-propanol[b]	pinacolyl alcohol (2,2-dimethyl-3-butanol)
ketone	acetone[b]	methyl isobutyl ketone (MIBK)	
organophosphorus compound	dimethylmethylphosphonate (DMMP)	diisopropylmethylphosphonate[b] (DIMP)	tributyl phosphate (TBP)
water[b]			

[a] Kerosene is typically a mixture of *n*-dodecane, several alkyl derivatives of benzene, naphthalene, and a pair of tetrahydronaphthalenes (Windholz, M., Ed., *The Merck Index*, 10th ed.; Merck & Co.: Rahway, NJ, 1983). [b] These compounds were used to form binary mixtures.

semiconductors,[15] and porous oxides.[16] Our long-term goal is to assemble of a "library" of chemically sensitive interfaces whose responses to a range of vapors and gases are characterized, allowing selection of the best subset of materials for a particular application scenario. The examples presented below rely primarily upon data obtained from SAMs, PGFs, and PPFs.

Self-assembled monolayers show promise for a diverse set of thin-film applications ranging from chemical sensors to model biological membranes.[9] The 1-alkanethiol-based SAMs, described and characterized elsewhere in detail,[17] provide a simple, reproducible, relatively well-ordered materials platform to support a chemically diverse collection of tail groups. We have studied SAMs formed from $HS(CH_2)_{15}CH_3$, $HS(CH_2)_2SO_3H$, $HS(CH_2)_{10}COOH$ (MUA), $HS(CH_2)_{10}COO^-$ coordinated to Cu^{2+}, Ni^{2+}, Fe^{2+}, and Zr^{2+}, $HS(CH_2)_9CN$, and $HS(CH_2)_9NH_2$. SAM formation on SAW devices is reported elsewhere.[1]

We examine two types of plasma-processed films. PGFs are a promising new class of polymeric materials with the potential to incorporate a wide range of functional groups in an open and permeable polymer matrix.[11] A brief exposure of the substrate to a gas-phase plasma of the appropriate monomer produces a thin cross-linked polymer "base layer" with a relatively stable population of free radicals; with the plasma switched off, an (unsaturated) molecule to be grafted is introduced and undergoes free-radical polymerization, resulting in a "kelp-forest-like" grafted layer with few cross-links.[1] Polymerization ceases as free radicals are removed via radical recombination of two adjacent chains or by a quencher (impurity O_2 or H_2O). We have utilized isobutylene and acrylic acid to form base layers, with acrylic acid used for grafts. Such films *do not* have the ordered nature of SAMs: there is no epitaxy, and as the chains grow, they can fold and connect to one another. Their advantage is a high density of the desired functional group in a relatively permeable thin film, complementing the well-packed, relatively impermeable alkanethiol-based SAMs, where interactions are primarily with the tail groups.

Some species, despite vinyl functionalities or other unsaturations, do not readily graft onto the base layers. For these, PPFs can be formed[18] from a wide range of monomers that include many different functional groups. PPFs are relatively highly cross-linked due to the proliferation of free radicals in a plasma discharge, so film thickness must be minimized if analyte permeation is to be rapid. We have characterized the response of SAW devices coated with plasma-polymerized eugenol (2-methoxy-4-(*2*-propenyl)phenol) and vinylphosphonic acid films.[18]

The SAW Transducer Platform[2]

Any change in a physical property of a thin film on the SAW device surface that affects SAW velocity or attenuation is the basis for a chemical sensor; changes in pressure, temperature, mass, film mechanical properties, electrical conductivity, and dielectric coefficient can all affect the SAW. In practice, most SAW-based chemical sensors rely upon their superior mass sensitivity to surface mass changes: a resolution of 100 pg/cm^2, corresponding to about 10^{-3} monolayer of $C_7H_{15}SH$, is not uncommon.

To monitor changes in SAW propagation characteristics, an oscillator loop is often utilized, as depicted in Figure 2.[2] In this circuit, the SAW device is the frequency-control element, frequency changes being proportional to velocity shifts:

$$\frac{\Delta f}{f_0} = \kappa\frac{\Delta v}{v_0} = -\kappa c_m f_0 \Delta(m/A) \qquad (3)$$

in which f_0 is the unperturbed oscillation frequency, v_0 is the unperturbed SAW velocity, κ is the fraction of the center-to-center distance between transducers being perturbed, c_m is the coefficient of mass sensitivity, and $\Delta(m/A)$ is the change in mass/area on the surface. The 97-MHz, ST-cut, *X*-propagating quartz SAW delay lines used in this work cause loop oscillation at 97 MHz; frequency stability (over several seconds) of better than 1 Hz is typical.[14] Thus, a frequency change of 1 part in 10^8, and a similarly small velocity change, is measurable. This measurement accuracy, combined with the distribution of the SAW energy within one acoustic wavelength of the surface,[2] provides the SAW's exquisite sensitivity to surface perturbations.

Analytes and SAW Array Responses

The present study focuses on the vapors of organic analytes representing various environmental pollutants, common industrial solvents, and chemical weapons simulants and precursors, as well as relative humidity. The analytes are grouped according to categories in Table 1. We have also characterized the responses from binary mixtures of seven of these compounds.

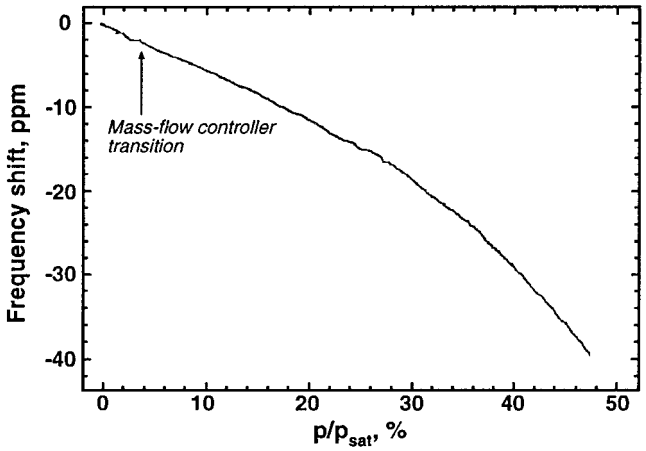

FIGURE 3. SAW-measured adsorption branch of a wide-concentration-range DIMP isotherm from 0.05 to 50% of p_{sat} (460 ppb to 460 ppm by volume). The SAW frequency shift is reported in parts per million (1 ppm of frequency shift = 97 Hz).

Because SAW devices respond to many perturbations, it is unwise to assume a linear relationship between analyte concentration and frequency shift. In addition, pattern-recognition (PR) results are generally valid when the number of data points for each chemical is several times the number of elements in the array.[19] We therefore measured wide-concentration-range isotherms[20] (including sorption and desorption branches), consisting of several hundred data points vs vapor-phase concentration, for every analyte and every film. A pair of mass-flow controllers provided N_2 to entrain the organic vapors, producing concentrations over the 0.05−50% of saturation vapor pressure (p_{sat}) range.

Figure 3 shows the adsorption branch of a typical "wide-range isotherm", in which the concentration of diisopropylmethylphosphonate (DIMP) is smoothly swept over the course of 2 h from 0.05% to 50% of its p_{sat} (0.7 Torr[21]). The chemically sensitive interface for this measurement is a SAM based upon $HS(CH_2)_{10}COO^-$ coordinated to Cu^{2+}, which is selective for organophosphonates.[10,21] The response is not linear, so a many-point isotherm is necessary.

Figures 4 and 5 show 1-propanol and toluene adsorption isotherms for six SAW devices monitored in parallel; three are coated with SAMs, two with PGFs, and one with a PPF, as specified in the figure caption. Again, the isotherms are not generally linear. The nonmonotonic behavior in one of the toluene isotherms between 30% and 50% of p_{sat} is likely an acoustic relaxation (resonance) effect in this film.[2,22]

Using the six films from Figures 4 and 5, plus three more (a second $HS(CH_2)_{15}CH_3$ SAM, a 15-min acrylic acid PGF on a 1-min poly(isobutylene) base layer, a 15-min acrylic acid PGF on a 5-min acrylic acid base), similar isotherms were obtained for all analytes listed in Table 1, apart from kerosene, TBP, and MIBK. With sorption isotherms from 9 different film-coated SAW devices for 13 analytes in hand, we sought the optimal combinations of films to form sensor arrays.

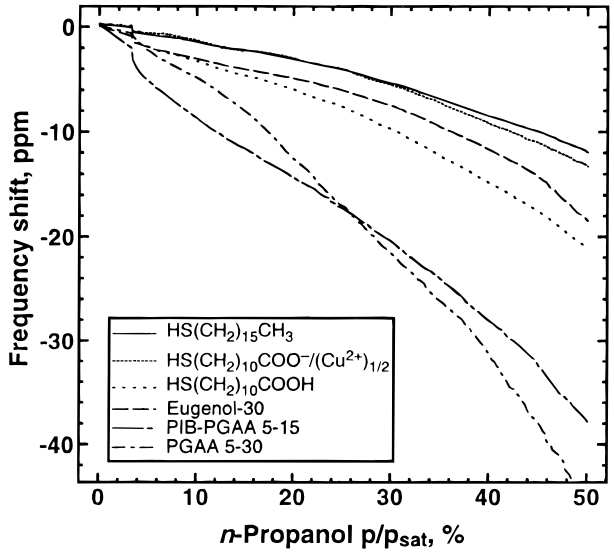

FIGURE 4. Sorption isotherms for 1-propanol on six SAW devices bearing chemically sensitive films as indicated in the legend. Eugenol-30 is a 30-min PPF of eugenol, PIB−PGAA 5−15 is a 15-min PGF of acrylic acid on a 5-min PPF isobutylene base layer, and PGAA 5−30 is a 30-min PGF of acrylic acid upon a 5-min PPF acrylic acid base layer. The response was measured only above p/p_{sat} = 3%.

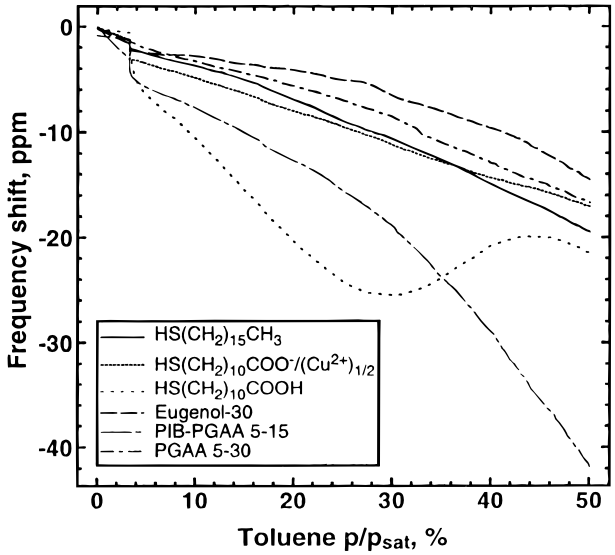

FIGURE 5. Sorption isotherms for toluene on six SAW devices, bearing the same chemically sensitive films described in Figure 4.

Array Optimization

Given a set of chemically independent materials, the next step is to find the smallest subset (array) that unambiguously identifies the expected analytes over the anticipated concentration ranges with anticipated levels of noise and drift. The most objective means of selection is to examine every combination having n or more elements, where n is the minimum desired array size, choosing the array that makes the fewest errors. This approach is practical when the number of available films, N, is not large (e.g., $N <$ 20); for large N, an optimization-search technique is needed to find probable best combinations without evaluation of all possibilities.

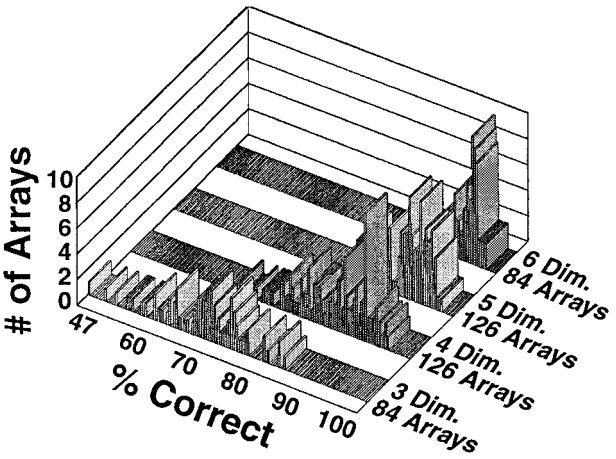

FIGURE 6. Sets of histograms showing the accuracy of VERI PR for different combinations of nine chemically sensitive films for which sorption isotherms were obtained on SAW devices. All analytes in Table 1, apart from kerosene, TBP, and MIBK, were examined. The front row is for three-film SAW arrays, the next row for four-film arrays, and so forth; at the right of each histogram, the number of possible combinations of the nine films is indicated. The heights of the bars represent the number of arrays that yield a particular percentage of correct identifications from all measured concentrations of 13 different analytes. The best performance, 98.3% correct identification, is provided by only 2 of the 84 possible six-film arrays.

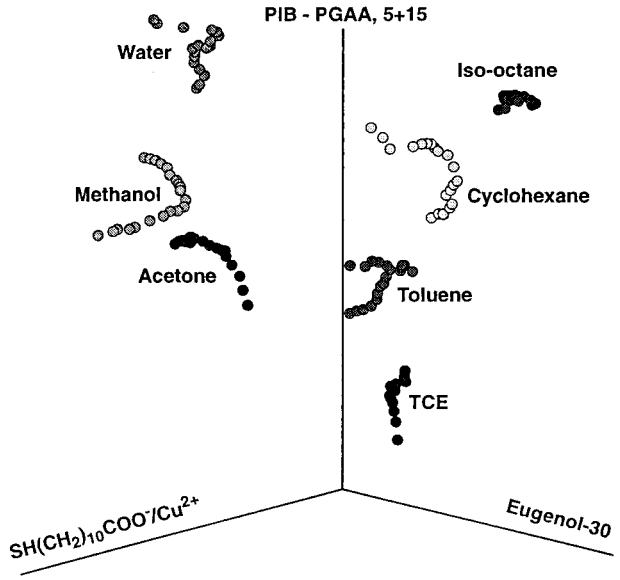

FIGURE 7. Graphic representation of clusters of points associated with several analytes for one of the best three-film arrays from Figure 6. The three axes represent the frequency shifts from SAW devices coated with $HS(CH_2)_{10}COO^-/(Cu^{2+})_{1/2}$, a 15-min acrylic acid PGF (on a 5-min poly(isobutylene) base layer), and a 30-min PPF of eugenol. Each point in the cluster for a given chemical represents a different concentration. Data are equalized, retaining only the directional information (all points are equidistant from the origin). This chemically diverse set of three films effectively separates the responses from the seven analytes shown. Addition of the remaining six analytes (from the group in Figure 6) results in noticeable overlap of some clusters, leading to uncertainties in identifying some concentrations of some analytes.

Results from our arrays of chemically modified SAW devices were analyzed using visually empirical region-of-influence (VERI) PR algorithms developed at Sandia National Laboratories (SNL).[23] Objective array optimization is a key strength of the VERI PR algorithms. Figure 6 summarizes the results. The heights of the bars in the histograms show the number of arrays producing a given percentage of correct classifications, i.e., unambiguous identification of a chemical species. The goal is to find one or more arrays that produce 100% correct results. To the right of the histograms, the number of SAW devices comprising each hypothetical array is indicated, along with the number of such arrays that can be constructed from every possible combination of the nine sensitive films. As detailed in refs 23 and 25, optimization relies on the objective, "brute-force" approach of examining all possible film combinations for all concentrations of all analytes. To learn whether a misidentification will occur, each data point is temporarily omitted from the training data and then presented to the algorithm as an unknown test point.

For the three-SAW arrays, none of the combinations of nine films yields a "perfect score"; the best outcome is a correct identification rate of 84%, provided by only 1 of the 84 possible combinations. When the size of the array is expanded to four, 1 of the 126 possible arrays correctly identifies 95.8% of the concentration-dependent data for the 13 analytes. The accuracy of the best arrays increases marginally thereafter, with one of the five-film arrays giving 97.9% and two of the six-film arrays yielding 98.3% accuracy. Note that the less-than-100% accuracy of the four-, five-, and six-element arrays is not due to misidentification; rather, a few points are classified as "outliers" by the PR algorithm because they lie far from the main clusters for their chemical class.

Figure 7 shows the results from one of the best three-film combinations of Figure 6. The axes represent the responses from three films identified in the caption. Each point in a given cluster represents a different concentration. The clusters do not approach the origin, even at low concentrations, because the data were equalized so that only directional information was retained, all points being equidistant from the origin. The 16% error rate associated with this three-film set is not apparent in Figure 7 because overlapping chemicals were omitted for clarity; the error rate is 0% for those analytes depicted. We point out that if the responses from the three films of Figure 7 were linear, the cluster for each chemical would collapse to a single point. VERI PR, like the human visual recognition upon which it is based, however, works as well with unusually shaped, nonlinear clusters as with linear data.[23−25] Notably, of the three materials categories (SAM, PGF, and PPF), the best-performing three-dimensional array contains one film from each category. This demonstrates that thin-film diversity leads to the most effective arrays.

Once an analyte is correctly identified, concentration is the next concern. This is accomplished separately from identification, by "looking up" the original training data from all of the sensors in the array. We believe a voting/averaging scheme, whereby the one or two responses

furthest from the mean are discarded and the remaining concentrations averaged, will be most effective.

Chemical Mixtures

Seven chemicals identified in Table 1 (one from each category) were selected to form 21 binary mixtures. A "double isotherm" was obtained for each mixture: the concentration of one analyte started at 0.3% and the second at 50% of p_{sat}, and then the concentrations were smoothly swept over the course of 2 h in opposite directions until the first analyte reached 50% and the second 0.3%; the concentrations were then swept back to the starting values. While they do not cover all possible concentration combinations, these data include the extrema where the concentration of one analyte is high and the other low, as well as the situation where the concentrations are comparable. The data included isotherms also for the 7 individual chemicals, for a total of 28 distinct chemical classes. Rather than repeating the array-optimization process, one of the best six-sensor arrays from the optimization of Figure 6 was selected; it included the three films of Figure 7, two additional SAMs (HS-$(CH_2)_{15}CH_3$ and MUA), and a 30-min PGF of acrylic acid (with 5-min acrylic acid base layer). Approximately 98%-accurate identification of the various concentrations of all 28 mixtures and compounds was achieved with this array.

Reproducibility, Noise, and Drift

Two important considerations when sensor array systems are applied outside the laboratory are the gradual change with time in the chemical sensitivity of a film as it ages, and increased noise levels due to inadequate control of temperature, pressure, humidity, etc. Ideally, only films exhibiting negligible aging would be selected for use in a practical system, but the ability of chemical identification algorithms to adapt to moderate changes in film sensitivity increases the number of candidate materials, in addition to enhancing the robustness of the sensor system to unexpected conditions. We therefore studied the effect of variations in film sensitivities on the accuracy of VERI PR.[23−25] The aging of sensing films was studied experimentally as well, with isotherms obtained for a given film/analyte combination periodically over the course of several months; in the intervening periods, films were exposed to many other analytes, as well as the laboratory ambient, so reproducibility data include the effects of exposure to a range of chemicals.

Figure 8 shows a series of isotherms, obtained monthly, for the adsorption of DIMP on a MUA SAM. The maximum deviation is roughly 25% of the signal at $p/p_{sat} = 5\%$, diminishing to about 12% at $p/p_{sat} = 50\%$. Assuming (modified) BET-type adsorption (stronger adsorption of the first monolayer, followed by multilayer condensation governed by the heat of vaporization of the bulk liquid[26]), we expect the most severe "aging" to occur at low surface coverage: contamination of the SAM and/or gradual changes in the details of its ordering[10] should most affect the energy of adsorption of the first monolayer or two.

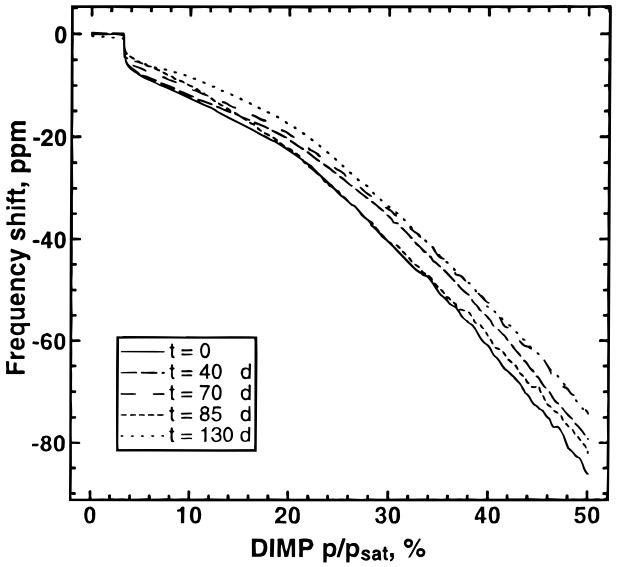

FIGURE 8. Adsorption isotherms, obtained at the indicated number of days after the initial experiment, for DIMP vapor in contact with a MUA SAM. The coated device was exposed to a wide range of other organic vapors and the laboratory ambient atmosphere between measurements. The maximum deviation is roughly 25% of the signal at $p/p_{sat} = 5\%$, diminishing to about 12% at $p/p_{sat} = 50\%$ (the data are unreliable below $p/p_{sat} = 4\%$ in this case).

Repeatability of the sort shown in Figure 8 is not obtained from every film, but a substantial percentage of the materials examined performed similarly.

An important measure of the robustness of a PR method is the accuracy of recognition in the face of such signal degradation; this is examined in Figures 9 and 10. Figure 9 shows results for a three-film array, the best subset from six tested films: two SAMs, based on SH-$(CH_2)_{15}CH_3$ and $HS(CH_2)_{10}COO^-/(Cu^{2+})_{1/2}$; two custom-synthesized fluorinated polyimides[12,27] (ca. 400 nm thick); a 47-nm-thick film of poly(*N*-vinylpyrrolidone);[27] and an unfunctionalized Au thin film. The analytes here included one or two representatives from each of the seven chemical categories in Table 1, as indicated by labels on the figure (unlike Figure 7, these data are not equalized, so the isotherms approach the origin as analyte concentrations diminish). Note that the best-performing array of Figure 9 includes the maximum film diversity: one metal, one fluorinated polymer, and one SAM.

In Figure 10, each of the original isotherms of Figure 9 is replaced by an expanded "band" of data, bounded above by the original data and below by the original data diminished in magnitude (in all three dimensions) by 25%. To include any amount of signal degradation from zero to 25%, the expanded band of data is filled with randomly selected points. Remarkably, these signal-degraded clusters provide 92%-accurate recognition of all concentrations of the analytes shown.

When the sort of array optimization depicted in Figure 6 is carried out on data that have been "degraded" as in Figure 10, another intuitive result is obtained: small arrays such as those represented by Figures 7 and 9 must be made larger (increasing to four, five, or six elements) to maintain high accuracy. We do *not* find, however, that

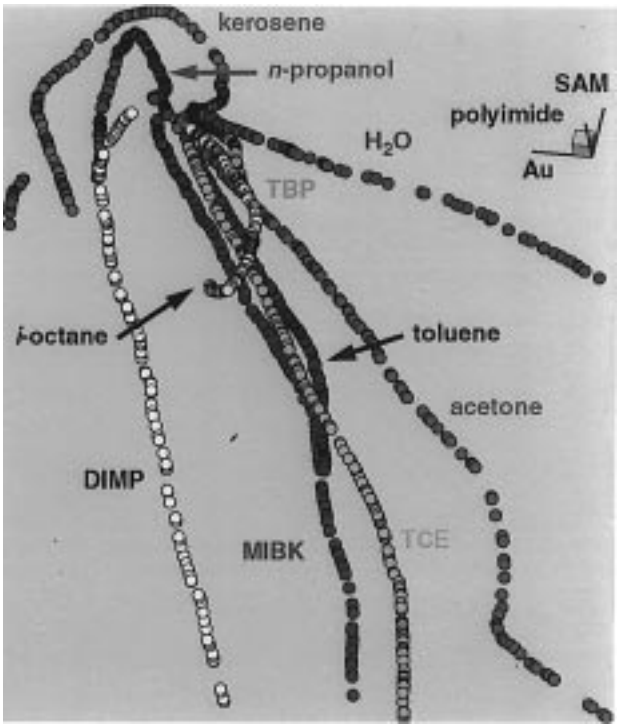

FIGURE 9. Graphic representation of clusters of points associated with 10 different analytes, as indicated in the figure (see Table 1 for abbreviations); the individual points represent different concentrations of each analyte. The three axes represent SAW frequency shifts from $HS(CH_2)_{10}COO^-/(Cu^{2+})_{1/2}$ (denoted "SAM"), a 400-nm-thick custom-synthesized fluorinated polyimide, and a bare Au film. These data, unlike Figure 7, are not equalized, so the strings of points (the isotherms) converge at the origin as concentrations approach zero.

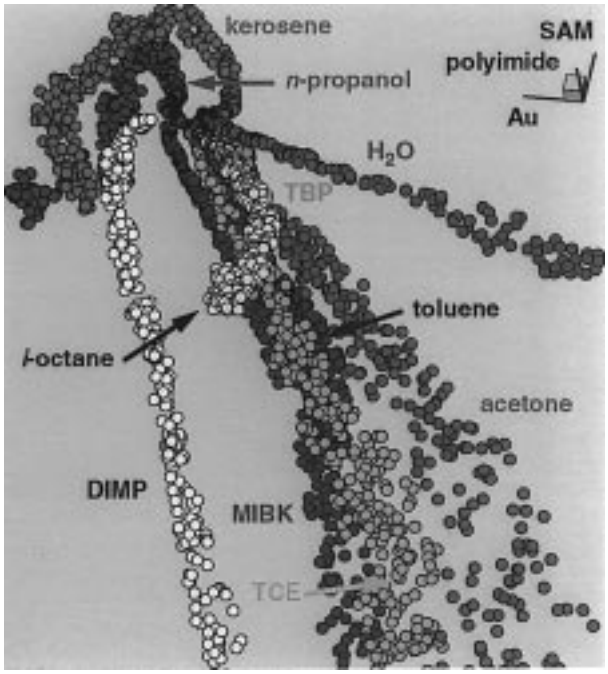

FIGURE 10. Results of Figure 9, with the mathematical addition of random error to diminish each response by 0−25% in all three dimensions. VERI PR maintains 92%-accurate recognition of all concentrations of the indicated analytes.

accuracy invariably improves as array size continues to grow:[23] there seems to be an optimum size, around five to seven films, beyond which recognition performance diminishes, particularly in the presence of degraded accuracy. Beyond a certain number, additional films do not add significant new chemical information, the consequence of their addition being instead the dispersal of the same information content over a larger number of dimensions. We qualify this conclusion by noting that the optimal upper limit on array size almost certainly depends on the degree of chemical diversity in the array: we have yet to examine a combination of films that draws, for example, simultaneously upon metals, ceramics, organic polymers, plasma-processed films, conducting polymers, molecularly organized films, and coordination complexes in a single array. Our expectation is that such increased diversity will increase the maximum optimal array size.

Conclusions and Outlook

To develop an effective chemical sensor array system of maximum performance with minimum size, weight, and cost, proper selection of chemically sensitive interfaces is critical. Accomplishing this task hinges on (1) the availability of a diverse set of *chemically independent* materials and (2) objective selection of the best film set for a particular problem. We believe the former problem is the more daunting, and progress in chemical sensors will continue to be paced by the development and characterization of suitable materials.

Our results confirm several intuitive hypotheses: (1) maximum chemical independence is often provided by films from very different materials families; (2) as sensor signal fidelity diminishes, array elements must be chosen carefully, in some cases increasing array size to minimize identification errors; (3) a relatively small array (three or four films), if the materials are sufficiently diverse and the responses stable, can reliably identify a large number of chemicals and mixtures. These conclusions are generally independent of the type of sensor platform.

The next generation of chemical sensor systems is likely to increase discrimination capabilities while maintaining or shrinking the number of sensor elements by (1) the use of heterogeneous arrays (different platform types and transduction techniques often provide the most chemically independent responses), (2) measurement of multiple physical parameters, e.g., mass and conductivity, for each chemically sensitive interface, (3) measurement of response kinetics, and (4) measurement of controlled extrinsic perturbation-dependent responses, for example, temperature or wavelength dependence. Clever use of such means to enhance array information content will lead to versatile, powerful sensor systems.

We gratefully acknowledge John W. Bartholomew for data analysis and PR graphics; Alan W. Staton for data acquisition; Ronald E. Allred, Brent Gordon, Andrea E. Hoyt, Ross C. Thomas, and Chuanjing Xu for preparation and characterization of chemically sensitive films; Stephen J. Martin for device and fixture design; and Mary-Anne Mitchell for device fabrication. R.M.C. acknowledges support under contract from SNL and the National Science Foundation (Grant CHE-9313441). Work at SNL was

supported by the United States Department of Energy (DOE) under Contract DE-AC04-94AL85000, with specific funding for this work from DOE/NN-20, for which we thank Michael O'Connell and his colleagues. Sandia is a multiprogram laboratory operated by Sandia Corporation, a Lockheed-Martin Company, for the United States Department of Energy.

References

(1) Ricco, A. J.; Xu, C.; Crooks, R. M.; Allred, R. E. In *Interfacial Design and Chemical Sensing*; Mallouk, T. E., Harrison, D. J., Eds.; ACS Symposium Series No. 561; American Chemical Society: Washington, DC, 1994; Chapter 23, pp 264−279.

(2) Ballantine, D. S.; White, R. M.; Martin, S. J.; Ricco, A. J.; Frye, G. C.; Zellers, E. T.; Wohltjen, H. *Acoustic Wave Sensors: Theory, Design, and Physico-Chemical Applications*; Academic Press: San Diego, 1997.

(3) Kovacs, G. T. A.; Petersen, K.; Albin, M. *Anal. Chem.* **1997**, *68*, 4407A.

(4) Harrison, D. J.; Fluri, K.; Seiler, K.; Fan, Z.; Effenhauser, C. S.; Manz, A. *Science* **1993**, *261*, 895.

(5) Jacobson, S. C.; Moore, A. W.; Ramsey, J. M. *Anal. Chem.* **1995**, *67*, 2059.

(6) Ballantine, D. S. Jr.; Rose, S. L.; Grate, J. W.; Wohltjen, H. *Anal. Chem.* **1986**, *58*, 3058.

(7) Grate, J. W.; Abraham, M. H. *Sens. Actuators, B* **1991**, *3*, 85.

(8) We assume here that all sensors and films are evaluated (and provide some response) over the same concentration range. However, in the instance that different films have different, (partially) nonoverlapping dynamic ranges, multiple films with functionally identical responses displaced from one another along the concentration axis can extend the dynamic range of the array.

(9) Swalen, J. D.; Allara, D. L.; Andrade, J. D.; Chandross, E. A.; Garoff, S.; Israelachvili, J.; McCarthy, T. J.; Murray, R. W.; Pease, R. F. *Langmuir* **1987**, *3*, 932.

(10) Thomas, R. C.; Yang, H. C.; DiRubio, C. R.; Ricco, A. J.; Crooks, R. M. *Langmuir* **1996**, *12*, 2239.

(11) Hsieh, Y. L.; Wu, M. *J. Appl. Polym. Sci.* **1991**, *43*, 2067.

(12) Hoyt, A. E.; Ricco, A. J.; Yang, H. C.; Crooks, R. M. *J. Am. Chem. Soc.* **1995**, *117*, 8672.

(13) Wells, M.; Crooks, R. M. *J. Am. Chem. Soc.* **1996**, *118*, 3988.

(14) Ricco, A. J.; Martin, S. J. *Thin Solid Films* **1991**, *206*, 94.

(15) Ricco, A. J.; Martin, S. J.; Zipperian, T. E. *Sens. Actuators* **1985**, *8*, 319.

(16) Frye, G. C.; Martin, S. J.; Ricco, A. J. In *Chemical Sensors and Microinstrumentation*; Murray, R. W., Dessy, R. E., Heineman, W. R., Janata, J., Seitz, W. R., Eds.; ACS Symposium Series No. 403; American Chemical Society: Washington, DC, 1998; Chapter 14.

(17) DuBois, L. H.; Nuzzo, R. G. *Annu. Rev. Phys. Chem.* **1992**, *43*, 437.

(18) To form PPFs of vinylphosphonic acid (Hoechst-Celanese) and eugenol (Polysciences), the monomers were held at 80 °C, entrained by a 5 L/min flow of Ar, and delivered into a continuously pumped quartz plasma-deposition chamber; all other conditions were as reported in ref 1 for PGF base layers.

(19) Duda, R.; Hart, P. *Pattern Classification and Scene Analysis*; Wiley & Sons: New York, 1973.

(20) Martin, S. J.; Ricco, A. J.; Ginley, D. S.; Zipperian, T. E. *IEEE Trans. UFFC* **1987**, *UFFC-34*, 142.

(21) Kepley, L. J.; Crooks, R. M.; Ricco, A. J. *Anal. Chem.* **1992**, *64*, 3191.

(22) Martin, S. J.; Frye, G. C.; Senturia, S. D. *Anal. Chem.* **1994**, *66*, 2201.

(23) Osbourn, G. C.; Bartholomew, J. W.; Ricco, A. J.; Frye, G. C. *Acc. Chem. Res.* **1998**, *31*, 297.

(24) Osbourn, G. C.; Martinez, R. F. *Pattern Recognit.* **1995**, *28*, 1793.

(25) Osbourn, G. C.; Bartholomew, J. W.; Bouchard, A. M.; Martinez, R. F. *Automated Pattern Recognition Based on the Visual Empirical Region of Influence (VERI) Method: A User's Guide*; http://www.sandia.gov/1100/1155Web/1155home.htm.

(26) Adamson, A. W. *Physical Chemistry of Surfaces*, 4th ed.; John Wiley & Sons: New York, 1982; Chapter XVI.

(27) Hoyt, A. E.; Ricco, A. J.; Bartholomew, J. W.; Osbourn, G. C. *Anal. Chem.* **1998**, *70*, 2137.

AR9600749